metals

MDPI

Article

Effects of Low Nickel Content on Microstructure and High-Temperature Mechanical Properties of Al-7Si-1.5Cu-0.4Mg Aluminum Alloy

Hongping Chen, Shusen Wu, Jianyu Li, Dijia Zhao and Shulin Lü *

State Key Lab of Materials Processing and Die & Mould Technology, School of Materials Science and Engineering, Huazhong University of Science and Technology, Wuhan 430074, China; ssw636@hust.edu.cn (S.W.)
* Correspondence: shulin317@hust.edu.cn

Abstract: In this paper, the effects of Ni content on the room and elevated temperature (250 °C) tensile strength of Al-7Si-1.5Cu-0.4Mg-0.3Mn-0.1RE-xNi (x = 0, 0.3, 0.6, 0.9 wt.%) alloys were investigated, along with microstructure characterization and tensile testing. In the as-cast state, the dominant Ni-rich phases were primarily the γ-Al7Cu4Ni and δ-Al3CuNi phases. Following the solution heat treatment, a significant reduction in the γ-Al7Cu4Ni phase was noted, accompanied by the emergence of numerous small ε-Al3Ni phases. Both room temperature strength and high temperature strength at 250 °C exhibited a consistent increase with rising Ni content, reaching 405 MPa and 261 MPa, respectively, at 0.9 Ni content, which were increased by 6.4% and 16.8%, respectively, compared with 0 Ni content. The elongation exhibited an oscillating increase within the Ni content range of 0 to 0.6, reaching peak values of 2.6% in room temperature and 4.3% in high temperature at 0.6 Ni, followed by a rapid decline. At 0.6 Ni content, the alloy demonstrated a well-balanced combination of mechanical properties, featuring commendable strength and plasticity.

Keywords: Al-Si-Cu-Ni alloy; Ni content; high-temperature mechanical properties; microstructure

check for updates

Citation: Chen, H.; Wu, S.; Li, J.; Zhao, D.; Lü, S. Effects of Low Nickel Content on Microstructure and High-Temperature Mechanical Properties of Al-7Si-1.5Cu-0.4Mg Aluminum Alloy. *Metals* **2024**, *14*, 223. https://doi.org/10.3390/met14020223

Academic Editors: Amogelang Bolokang and Noé Cheung

Received: 10 January 2024
Revised: 5 February 2024
Accepted: 8 February 2024
Published: 12 February 2024

Copyright: © 2024 by the authors. Licensee MDPI, Basel, Switzerland. This article is an open access article distributed under the terms and conditions of the Creative Commons Attribution (CC BY) license (https://creativecommons.org/licenses/by/4.0/).

1. Introduction

On the premise of ensuring the strength and safety performance of the vehicle, the application of lighter materials to replace traditional steel and other automobile structural components can reduce the overall vehicle weight, which can effectively improve the vehicle's power performance, reduce fuel consumption and exhaust pollution. The Al-Si multi-components alloy, characterized by high strength, low density and good castability, emerges as an ideal lightweight material for transportation [1,2]. With the development of the modern automobile industry, there is a growing trend toward higher power density in engines. Components such as engine pistons and cylinder blocks operate under prolonged exposure to high temperatures and pressures, placing elevated demands on the comprehensive properties of materials at elevated temperature to achieve the objectives of higher power density [3].

Alloying proves to be an effective approach for enhancing the properties of Al-Si alloys. Al-Si-Cu-Mg alloys formed by incorporating elements like Cu and Mg exhibit good heat resistance [4–6] and find widespread application in the manufacturing of engine components, exemplified by A380, 319 alloys [7–9]. In these alloys, the Al_2Cu phase is the primary heat-resistant strengthening phase. Nevertheless, the Al_2Cu phase will rapidly coarsen when the working temperature surpasses 250 °C [10], due to its lower thermal stability, which will lead to a significant deterioration in its high-temperature performance. At elevated temperatures, the strength of alloy grain boundaries significantly decreases, and so their resistance to dislocation motion reduces, and the plastic deformation mode shifts towards high-temperature diffusion deformation [2]. The fracture

mechanism transitions from a transgranular fracture to an intergranular fracture. Consequently, the presence of high-temperature-stable second-phase particles distributed along grain boundaries increases the resistance to plastic deformation, playing a role in enhancing the high-temperature strength of the alloy. Several studies suggest that the incorporation of Ni elements into Al-Si-Cu-Mg alloys can form various heat-resistant intermetallic phases, such as the ε-Al_3Ni phase, the δ-Al_3CuNi phase and the γ-Al_7Cu_4Ni phase. Researchers have conducted studies on the characteristics of these phases and their effects on the alloy. Z. Asghar et al. proposed that the mechanical performance of the alloy at high temperatures is significantly influenced by the three-dimensional mesh structure of these phases, and the impacts of these three phases vary [11–14]. The Cu/Ni ratio exhibits a strong correlation with both the type and quantity of the Ni-rich phase [15–18]. In instances of Cu content levels that are comparatively low, the predominant Ni-rich phase is typically a strip-like ε-Al_3Ni. With increasing Cu content, the network-shaped δ-Al_3CuNi becomes the primary Ni-rich phase, followed by γ-Al_7Cu_4Ni. Suwanpreecha et al.'s research indicated that the Al_3Ni phase has good heat resistance at 300 °C [19]. The high-temperature fatigue test by Feng et al. showed that the stability of the ε-Al_3Ni phase persists even at 350 °C and is beneficial to the alloy's elevated temperature performance [20]. Li et al. investigated quantitatively the contributions of δ-Al_3CuNi, ε-Al_3Ni and γ-Al_7Cu_4Ni phases to high-temperature performance [15]. They determined that the network-shaped δ-Al_3CuNi phase contributes the most, followed by the γ-Al_7Cu_4Ni phase in a closed or semi-closed loop-shaped configuration, and lastly, the strip-like ε-Al_3Ni phase. Other literature also reported that the δ-Al_3CuNi phase has the most noteworthy influence on high-temperature performance [16]. However, the Ni content in the above studies was relatively high.

There have been several relevant research reports on the impact of adding Ni to the Al-Si-Cu-Mg alloy. In these studies, the quantity of added Ni exceeded 1%, and the research results indicated that incorporating Ni elements to create Ni-rich phases could enhance the elevated temperature mechanical performance of the alloy. However, due to the high hardness and brittleness of Ni-rich phases, they may split the matrix structure, weakening the alloy's room temperature mechanical properties [21]. Studies with Ni content below 1% are relatively scarce. A lower Ni content results in relatively fewer Ni-rich phases, reducing the adverse impact on room temperature mechanical properties. Simultaneously, it may enhance the alloy's high-temperature performance to a certain extent and may achieve a favorable combination of room-temperature and high-temperature properties. This study explores the influence of different Ni addition amounts (wt.% = 0, 0.3, 0.6, 0.9) on the microstructure and mechanical properties of the Al-7Si-1.5Cu-0.4Mg alloy at both room temperature and 250 °C elevated temperature when the Ni addition amount is less than 1%.

In our previous research on Al-Si alloys, it was found that the addition of an appropriate amount of rare earth (RE) can effectively refine eutectic silicon [22]. Simultaneously, RE can form thermally stable compounds with elements such as Si, Cu, Mg, and Mn in the alloy, enhancing the high-temperature mechanical properties of the alloy. However, an excessive amount of RE (>0.3%) can lead to the formation of numerous needle-like RE compounds, thereby reducing the mechanical performance of the alloy. Therefore, in this study, we consider the addition of 0.1% RE to the alloy to enhance its high-temperature mechanical properties. Furthermore, in the melting of aluminum alloys, Fe is often an unavoidable impurity element. The needle-like Fe-rich phases formed can cleave the alloy matrix, thereby reducing the mechanical performance of the alloy. The addition of Mn elements can improve the morphology of the needle-like Fe-rich phases and mitigate their impact on the mechanical properties of the alloy [23–26]. Therefore, this study also considers adding an appropriate amount of Mn element to improve the morphology of the Fe-rich phase.

2. Materials and Methods

Aluminum alloys with designated compositions of Al-7Si-1.5Cu-0.4Mg-0.3Mn-0.1RE-xNi, with x values of 0, 0.3, 0.6, 0.9 (wt.%), were formulated, with 0.15% Ti as the grain refiner. The alloy's chemical composition is outlined in Table 1. The raw materials were Al-25Si, Al-10Mn, Al-5Ti and Al-10RE (RE is composed of 68% Ce and 32% La) master alloys, as well as commercial pure Al, pure Ni, pure Cu and pure Mg. The raw materials were melted using a resistance furnaces and graphite crucible of 3 kg capacity. After the alloy was melted, high-purity Ar gas (99.99%) was used for rotational degassing and refining for 15 min. Subsequently, the molten alloy was cast into a metal mold which was preheated to 200 °C, with temperatures in the range of 720 °C to 740 °C to form ingots with a size of $\Phi 30 \times 90$ mm^2.

Table 1. Chemical compositions (wt.%) of the alloys.

Alloy	Si	Cu	Mg	Mn	Ti	RE	Ni	Al
Ni0	7	1.5	0.4	0.3	0.15	0.1	0	Bal.
Ni0.3	7	1.5	0.4	0.3	0.15	0.1	0.3	Bal.
Ni0.6	7	1.5	0.4	0.3	0.15	0.1	0.6	Bal.
Ni0.9	7	1.5	0.4	0.3	0.15	0.1	0.9	Bal.

Samples for microstructure observations were taken from the identical position at the center of each ingot. After these samples underwent grinding, polished and etching with 0.5 vol% HF for 10 s, the alloy's microstructure was analyzed utilizing a Gemini SEM300 equipped with EDS. The alloy's phase composition was determined using a SHIMADZU XRD-7000S diffractometer (Shimadzu, Kyoto, Japan), covering a scanning angle range of 20 to 90 degrees at a scanning speed of 4°/min, and the samples were in powder form.

The mechanical performances of the alloys were tested following T6 heat treatment. The alloy underwent initial solution treatment at 530 °C for 7 h, followed by quenching in water at 70~80 °C, and finally aging at 190 °C for 10 h. Upon completion of the heat treatment, the samples were machined into standard rod-shaped tensile specimens, as illustrated in Figure 1, and underwent tensile tests at both 25 °C room temperature and 250 °C elevated temperature. Tensile testing was conducted using an MTS C45.105EY mechanical property testing machine (MTS Systems, Shanghai, China) equipped with a Haitham optical extensometer (Haitham, Shenzhen, China), operating at a testing speed of 2 mm/min. To ensure the precision of experimental data, the ultimate tensile strength and elongation after fracture were averaged from three repeated tests. The room temperature and high-temperature tensile methods, as well as specimen dimensions, complied with the GB/T228.1-2021 [27] and GB/T228.2-2015 [28] Chinese standards, respectively.

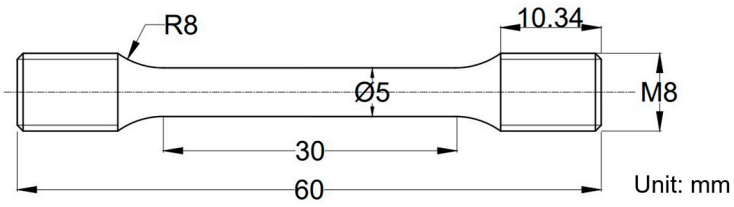

Figure 1. Schematic diagram of tensile specimen.

3. Results and Discussion

3.1. Microstructure of Al-Si-Cu-Mg Alloys with Low Ni Content

Figure 2 illustrates the alloy's SEM-BSE images with different Ni content. The alloy's microstructure predominantly consists of a dark α-Al matrix, eutectic Si phases, and bright complex second phases. When the Ni content is 0, the compound structures of the alloy are mainly the AlSiMnFe phase and the Al_2Cu phase. By incorporating the Ni element, Ni-rich phases appear in the alloy. Combining the element distribution of Cu and Ni

with the analysis results of the EDS point, as shown in Figure 3, the dominant Ni-rich phases are identified as the γ-Al_7Cu_4Ni phase and the δ-Al_3CuNi phase. The BSE image of the skeletal Ni-rich phase and its analysis results of the EDS point are presented in Figure 3a. The atomic ratio of Cu significantly exceeds that of Ni, indicating the presence of the skeletal γ-Al_7Cu_4Ni phase. Figure 3b displays the BSE image of the blocky Ni-rich phase along with its EDS point analysis result, where the atomic ratio of Ni and Cu is close to 1, indicating it is the blocky δ-Al_3CuNi phase. In the alloy containing 0.3% Ni (Figure 2b), the blocky γ-Al_7Cu_4Ni phase could be observed. In the alloy containing 0.6% Ni (Figure 2c), a strip-like γ- Al_7Cu_4Ni phase was observed. And, in the alloy with 0.9 Ni content (Figure 2d), both skeletal γ-Al_7Cu_4Ni and strip-like δ-Al_3CuNi phases are observed. These imply that the types of Ni-rich phases are associated with either the content of Ni or the Cu/Ni ratio.

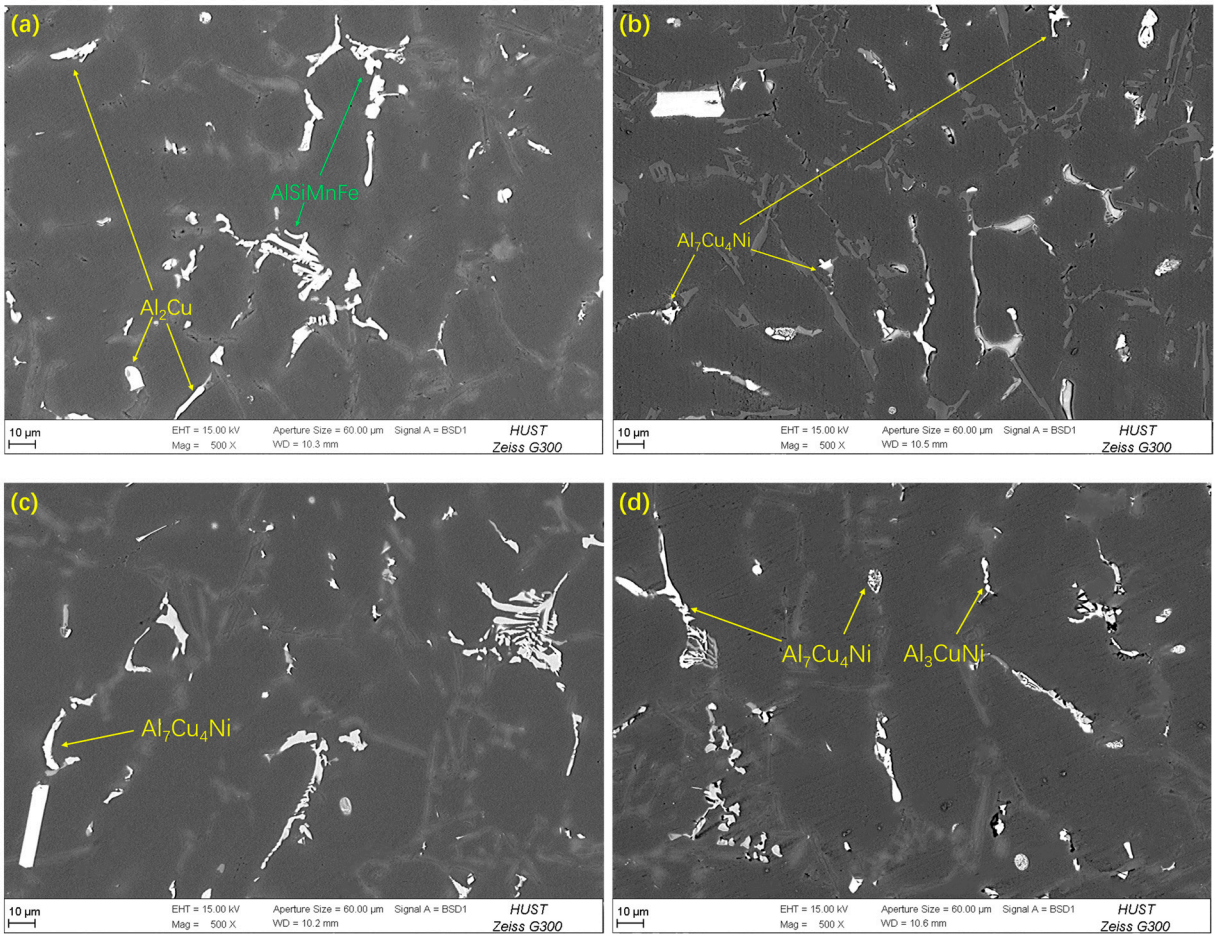

Figure 2. BSE images of alloy with different Ni content: (**a**) 0Ni, (**b**) 0.3Ni, (**c**) 0.6Ni, (**d**) 0.9Ni.

It is generally considered that in the Al-Si-Cu-Ni alloy, there are three main Ni-rich phases, namely the δ-Al_3CuNi, γ-Al_7Cu_4Ni and ε-Al_3Ni phases. The type and quantity of Ni-rich phases are highly correlated with the Cu/Ni ratio [15,16]. Different researchers have reported varied results regarding the morphology of Ni-rich phases. In the study by Liao et al. on Al-12%Si-4%Cu-1.2%Mn-x%Ni alloys, they observed that the δ-Al_3CuNi phase typically displays a skeletal or network-like structure, the γ-Al_7Cu_4Ni phase appears predominantly blocky, and the majority of ε-Al_3Ni phases are rod-like or needle-like [29]. In contrast, Li's research suggests that the δ-$_{Al3}$CuNi phase consistently displays a striped morphology, the γ-Al_7Cu_4Ni phase typically forms a skeletal structure, and the ε-Al_3Ni phase commonly exhibits a blocky morphology [30].

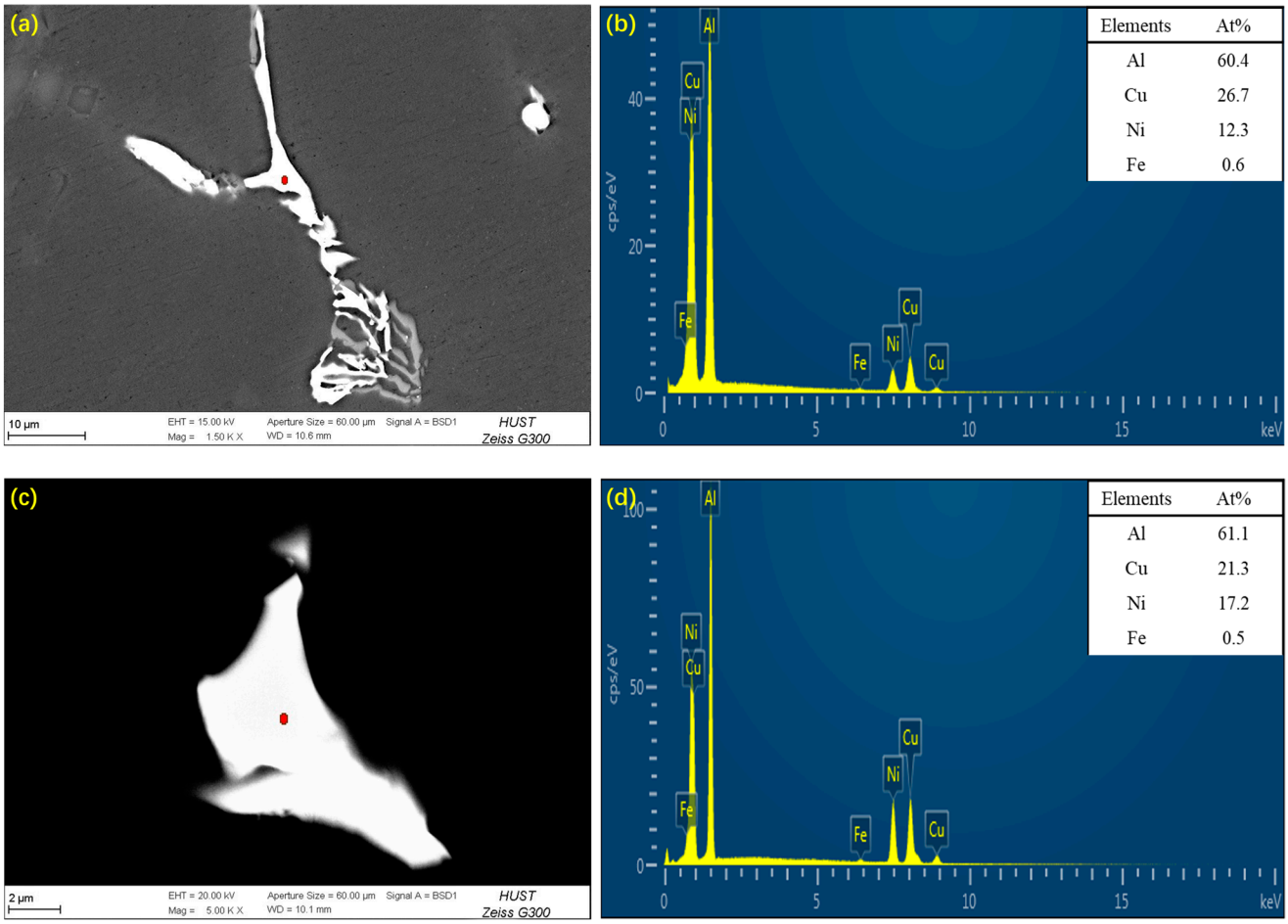

Figure 3. EDS result of Ni-rich phase: (**a**,**b**) skeleton-like Ni-rich phase in 0.9Ni alloy, (**c**,**d**) blocky Ni-rich phase in 0.9Ni alloy. (red dot means the EDS point position).

The δ-Al_3CuNi, γ-Al_7Cu_4Ni and ε-Al_3Ni phases still exhibit high stability at around 300 °C. These thermally stable intermetallic compounds are distributed at the grain boundaries, effectively enhancing the resistance to dislocation motion, thereby augmenting the alloy's high-temperature strength. Li et al.'s quantitative research shows that different types of Ni-rich phases have varying impacts on the alloy's elevated temperature properties [15]. The δ-Al_3CuNi phase contributes most to the high-temperature performance, followed by γ-Al_7Cu_4Ni, and lastly ε-Al_3Ni. This hierarchy is attributed to the superior volume utilization efficiency of the δ-Al_3CuNi phase in terms of its morphology. Yang et al.'s research considers that the high-temperature fracture of the alloy involves the intergranular ductile fracture [31]. At elevated temperatures, the α-Al matrix softens and can only play a role in transmitting the load. The features, morphology and fraction of the second phase with high strength at elevated temperatures are identified as the most crucial factors influencing the alloy's elevated temperature performance. The Ni-rich phases can impede the expansion of cracks and the sliding of grain boundaries, thereby improving the alloy's high-temperature strength. Z. Asghar et al. considered that the strength of the eutectic Al-Si alloy conforms to the reinforcement mechanism of fiber-reinforced composite materials [8]. The load is transferred from the pliable α-Al matrix to the sturdier eutectic Si phase, contributing to strengthening. The existence of robust and brittle Ni-rich phases, which exhibit high-temperature stability, aids in preserving the stability of the eutectic silicon network at elevated temperatures, thus enhancing the alloy's high-temperature performance.

The alloy's SEM-BSE images after T6 heat treatment are depicted in Figure 4. Due to the solution treatment, the Al2Cu phase in the matrix structure decomposes and disappears. Figure 5 shows the EDS point analysis results of the Ni-rich phase. The Ni/Cu atomic ratio is indicated, in Figure 5a, as a blocky-like ε-Al_3Ni phase and in Figure 5b as a striped-like δ-Al_3CuNi phase. After T6 heat treatment, the type and morphology of Ni-rich phase have some changes. In alloys with 0.3, 0.6, and 0.9 Ni content, a considerable amount of the ε-Al_3Ni phase is observed, along with some δ-Al_3CuNi phases. The ε-Al_3Ni phase is in the form of granules or blocks, with a few in the form of rods, and is dispersed throughout the alloy microstructure, with dimensions of only a few micrometers. The dimensions of the Ni-rich phase in the 0.9Ni alloy has increased, as depicted in Figure 4d. In contrast to the as-cast alloy's microstructure, more γ-Al_7Cu_4Ni phases and fewer ε-Al_3Ni phases are observed. It is speculated that in the T6-treated alloy, the increased presence the ε-Al_3Ni phase is likely due to the decomposition of the γ-Al_7Cu_4Ni phase during the solution treatment (530 °C × 7 h). While undergoing the solution process, Cu atoms dissolve into the Al matrix, the Cu/Ni ratio decreases, and the Ni element forms the ε-Al_3Ni phase. Then, the alloy undergoes swift cooling through quenching to attain room temperature, and the Cu atoms lack sufficient time for precipitation, preserving the ε-Al_3Ni phase. Zuo et al. used JMat-Pro software to calculate the thermodynamics of the solidification process on the Al-Si-Cu-Ni alloy, indicating that the ε-Al_3Ni phase formed at approximately 500 °C, and when the temperature dropped below 400 °C, the ε-Al_3Ni phase disappeared but the γ-Al_7Cu_4Ni phase and the δ-$_{Al3}$CuNi phase increased. That is, temperature will affect the type of Ni-rich phase in the alloy microstructure [32].

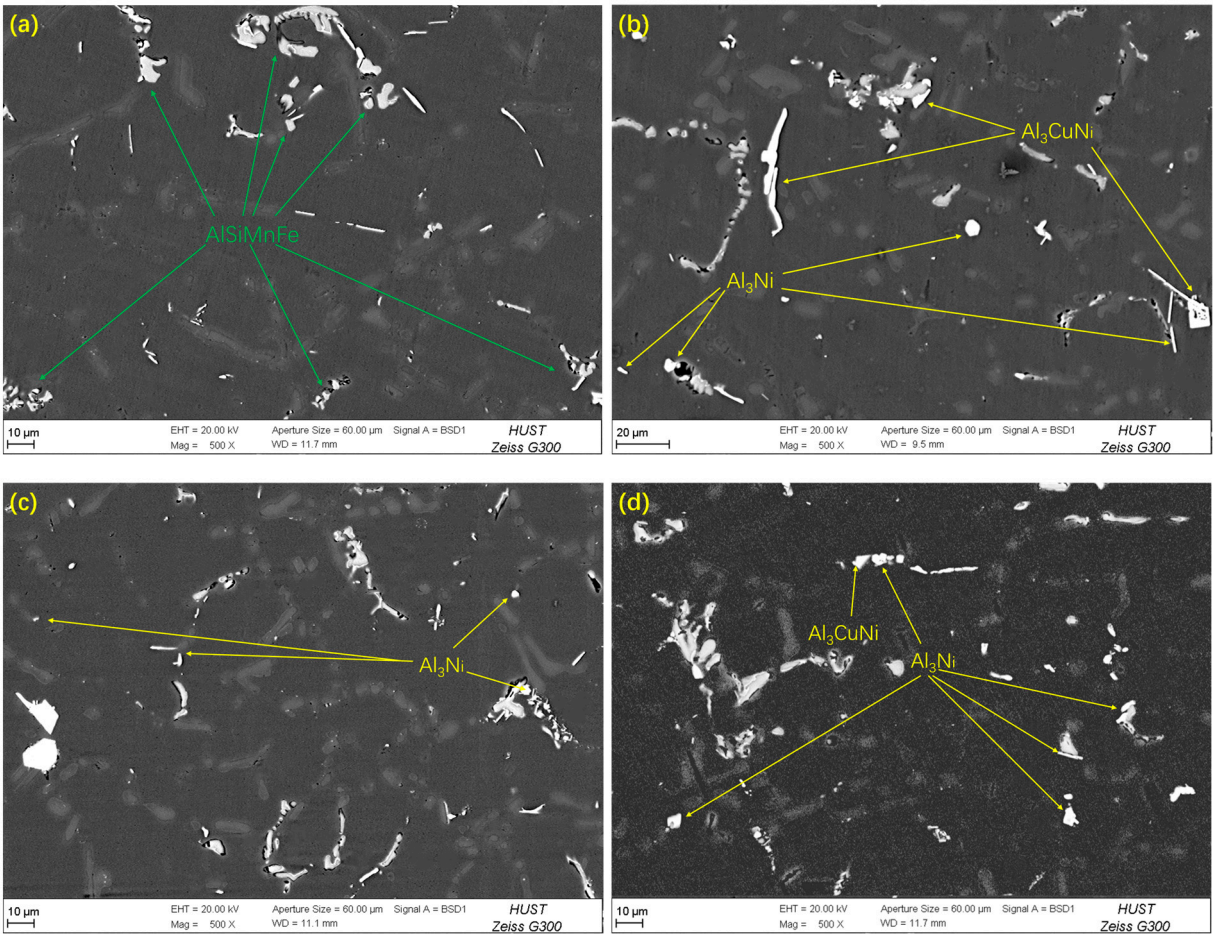

Figure 4. BSE images of alloy with different Ni content after solution: (**a**) 0Ni, (**b**) 0.3Ni, (**c**) 0.6Ni, (**d**) 0.9Ni.

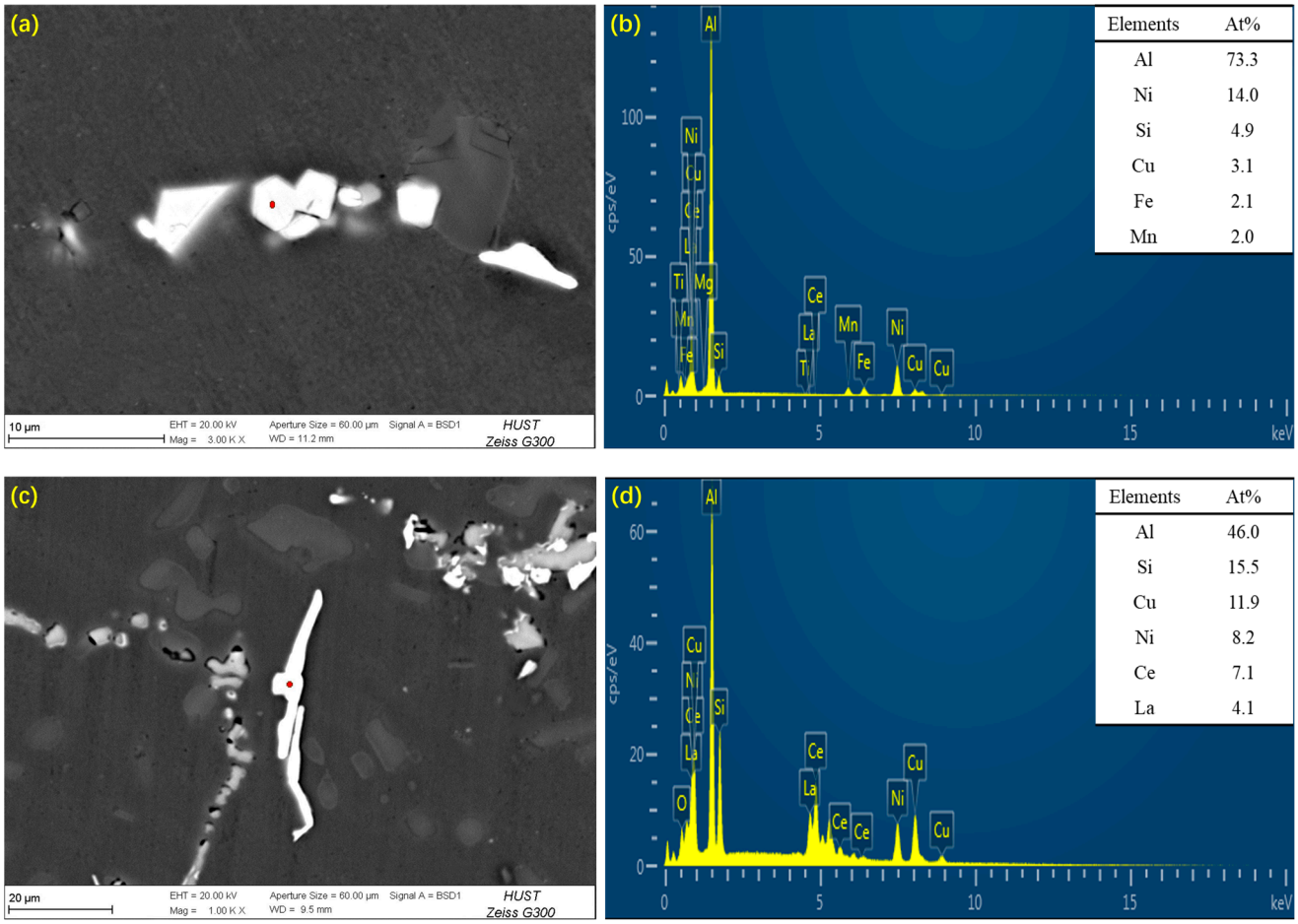

Figure 5. EDS result of Ni-rich phase in Figure 4: (**a,b**) blocky Ni-rich phase, (**c,d**) rod-like Ni-rich phase. (red dot means the EDS point position).

Figure 6 displays the XRD diffraction outcomes of alloys in both the as-cast and post-solution treatment states with varying Ni additions. The microstructure of the as-cast alloy with Ni addition comprises the γ-Al_7Cu_4Ni, δ-Al_3CuNi, and ε-Al_3Ni phases. Following solution treatment, the diffraction peaks related to the γ-Al_7Cu_4Ni phase vanish in the alloy containing 0.9% Ni. Cu element distribution in the as-cast and solution-treated state of the alloy with 0.9% Ni is depicted in Figure 7. Notably, numerous Cu-rich phases, including γ-Al_7Cu_4Ni and δ-Al_3CuNi phases, decompose during the solution process, with Cu elements dissolving into the matrix. The SEM images of the solution-treated state reveal an abundant dispersion of small-sized ε-Al_3Ni phases, the reduced presence of the δ-Al_3CuNi phase, and the absence of the γ-Al_7Cu_4Ni phase, further confirming the substantial decomposition of γ-Al_7Cu_4Ni and δ-$_{Al3}$CuNi phases during the solution treatment. Cu elements dissolve into the α-Al matrix, while Ni elements combine with Al to form the ε-Al_3Ni phase. For alloys with 0.6Ni and 0.3Ni additions, there are still weak diffraction peaks of the γ-Al_7Cu_4Ni phase in the XRD diffraction results of the alloys after solution treatment, and a multitude of small-sized and dispersed ε-Al_3Ni phases are also observed in their SEM images. This may be affected by the relatively high Cu/Ni ratio in low-Ni-content alloys, leading to a higher relative quantity of the γ-Al_7Cu_4Ni phase within the Ni-rich phases, which does not fully decompose during the solution treatment process.

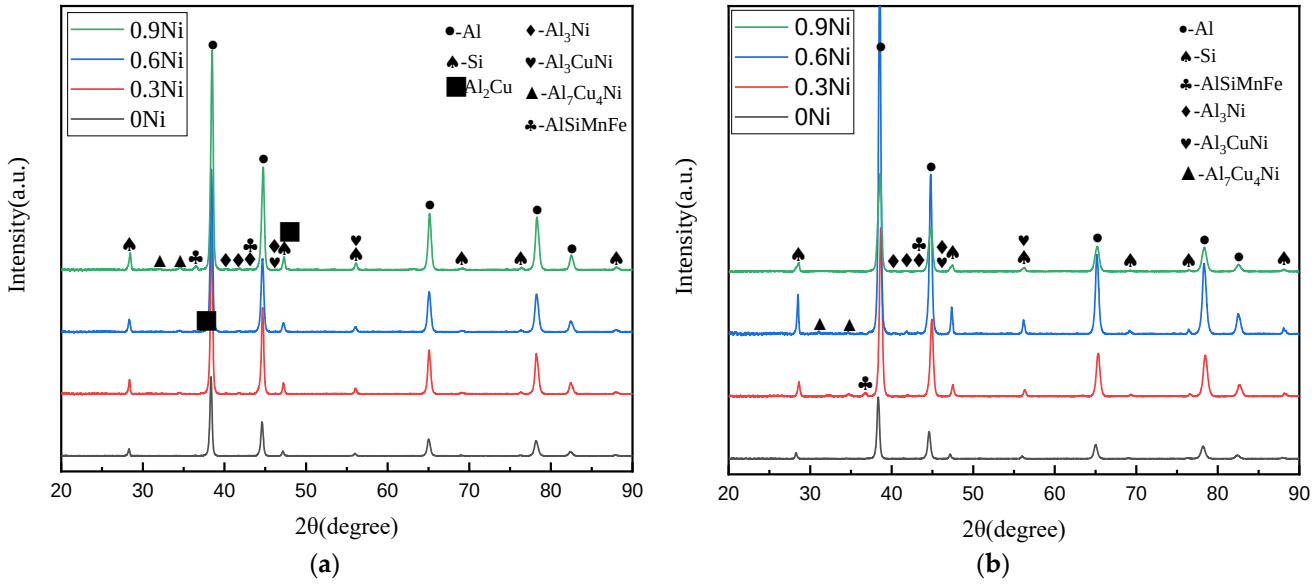

Figure 6. XRD diagram patterns of alloy with different Ni content: (**a**) as cast; (**b**) as solution.

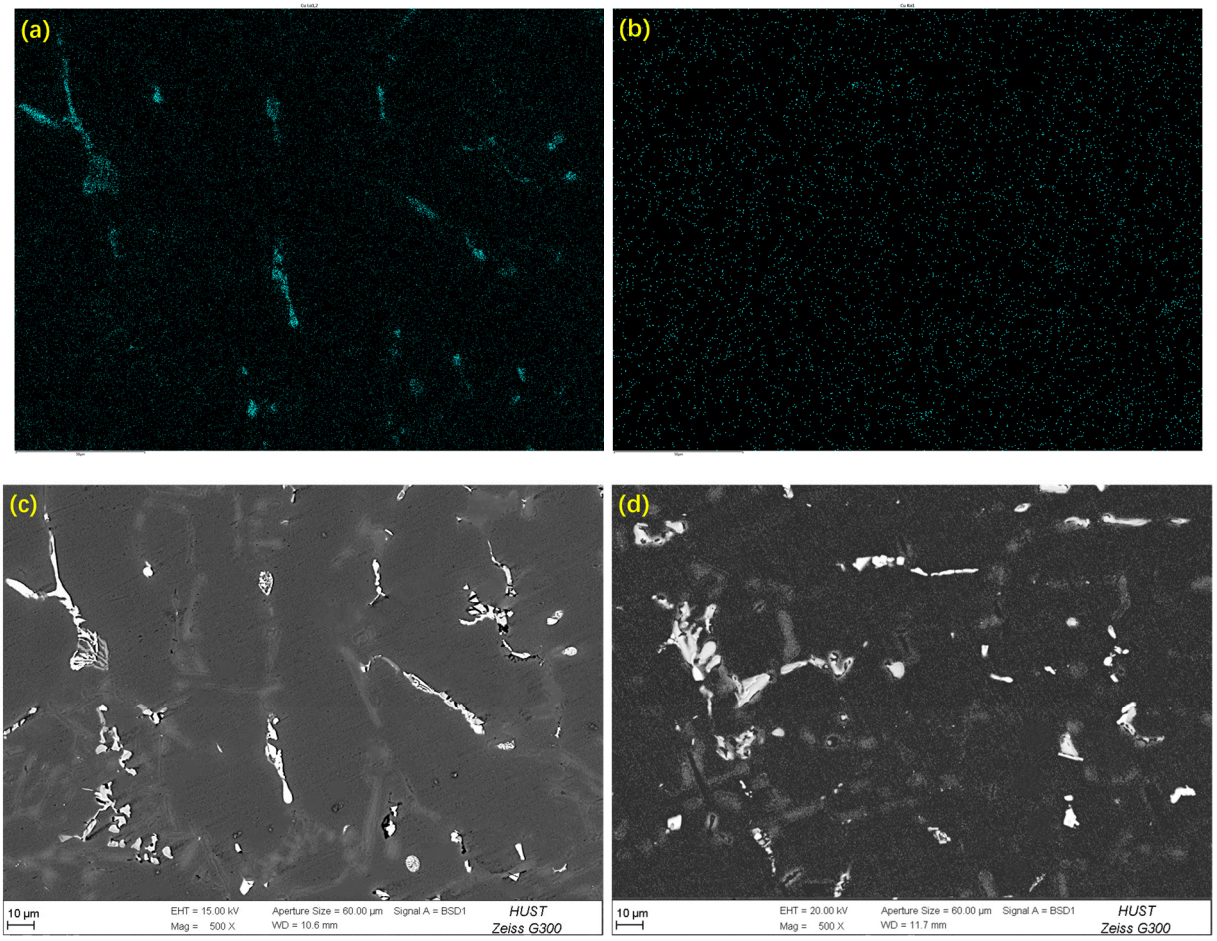

Figure 7. Elemental mapping distribution of Cu and BSE images in 0.9Ni alloy: (**a**,**c**) as cast, (**b**,**d**) as solution.

3.2. Mechanical Properties

Figure 8a,b illustrate, respectively, the variation curves of tensile properties at room temperature and 250 °C elevated temperature with different Ni contents for the investigated

alloy. Figure 8c illustrates the engineering stress–strain curve at room temperature. The investigated alloy, subjected to T6 treatment, exhibits excellent strength characteristics at room temperature, with tensile strength exceeding 380 MPa. Within the studied range of Ni addition, at room temperature, the tensile strength rises with an increase in Ni addition, and the rate of increase becomes more pronounced. At 0.9% Ni addition, the tensile strength achieves 405 MPa, indicating a 6.4% enhancement compared to the alloy with 0% Ni. The elongation at fracture initially increases, reaching its maximum at 0.6% Ni content, and then rapidly decreases. It is generally believed that at room temperature, the brittle Ni-rich phases will split the alloy matrix and weaken both its strength and plasticity. However, in this study, the formation of numerous ε-Al_3Ni phases after T6 treatment is characterized by small dimensions, typically only a few micrometers in size. The majority of these phases appear as well-rounded particles or blocky structures, dispersed throughout the alloy microstructure. Due to their favorable shape and distribution, these ε-Al_3Ni phases do not weaken the alloy's room-temperature properties. Instead, they interact with dislocations, hindering their movement and contributing to dispersion strengthening, resulting in a slight improvement in both strength and ductility. However, when the Ni addition is relatively high (>0.6%), the size of the Ni-rich phases within the alloy microstructure increases. The brittle and hard nature of these larger Ni-rich phases will restrict the deformation of the matrix structure, resulting in a rapid decline in the alloy's ductility.

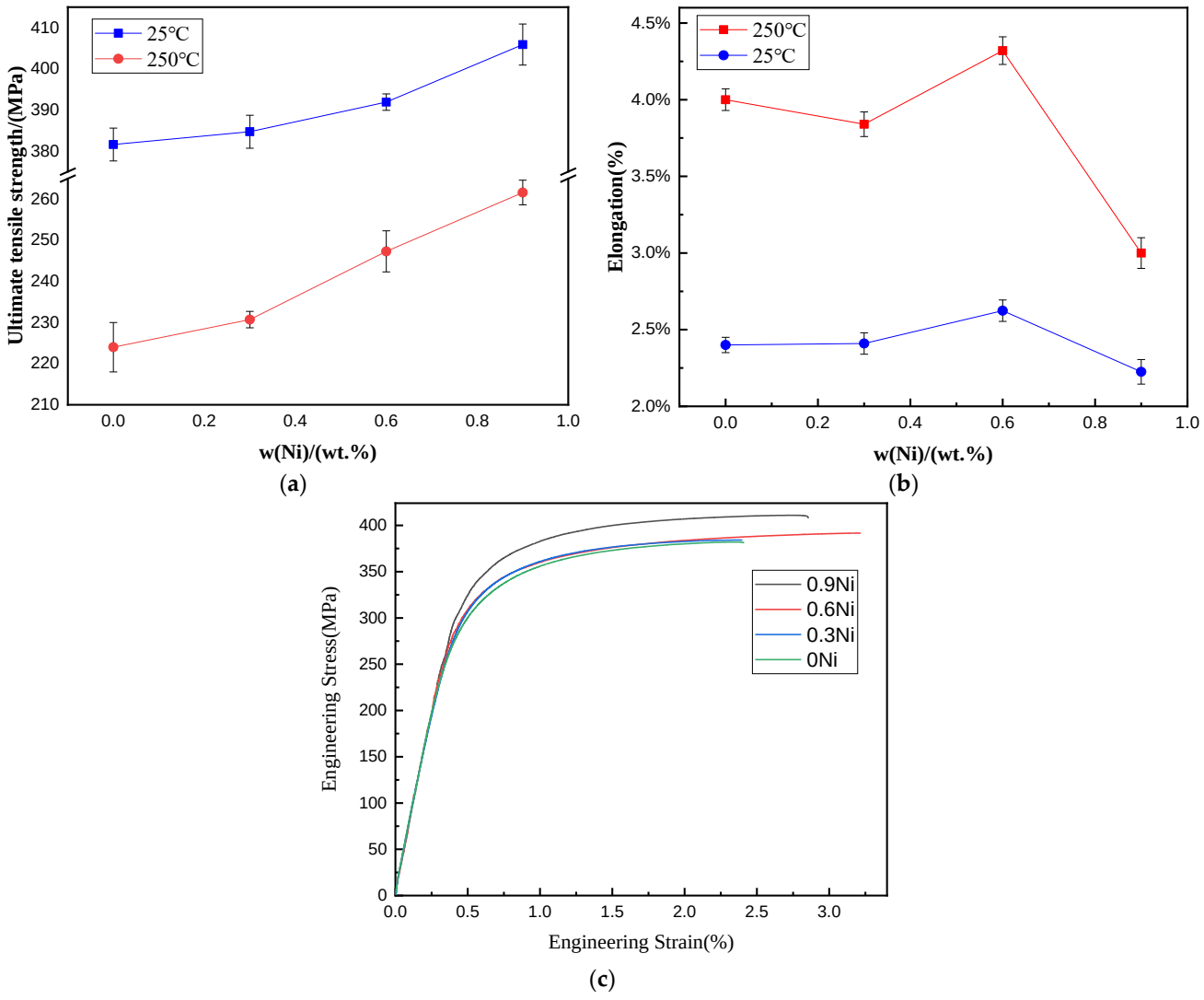

Figure 8. Tensile properties of the studied alloys with different Ni content after T6 treatment at different temperatures: (**a**) UTS, (**b**) EL. (**c**) Engineering stress–strain curve at room temperature.

At 250 °C, the investigated alloy continues to exhibit excellent strength characteristics, with tensile strength exceeding 220 MPa. Within the studied range of Ni addition, the tensile strength keeps rising with the increase in Ni content, reaching 261 MPa at 0.9Ni, which is 16.8% higher than that of the 0Ni alloy. With the increase in Ni content, the elongation at fracture exhibits an oscillating increase first, reaching its peak value at 0.6Ni, and then sharply decreases. At a high temperature of 250 °C, the high melting point means that Ni-rich phases can still maintain stability. These thermally stable Ni-rich phases are dispersed along the grain boundaries, augmenting the resistance to dislocation movement and consequently fortifying the alloy's elevated temperature strength. However, in the case of a high Ni addition (>0.6%), the brittle and hard nature of the Ni-rich phases will also limit the deformation of the matrix structure at high temperatures drastically, resulting in a sharp decrease in the alloy's ductility.

Zuo et al. investigated the impact of the ε-Al_3Ni phase on the mechanical properties of the Al-12Si-0.9Cu-0.8Mg alloy at room temperature and at 250 °C [33]. The findings indicate that at both room temperature and 250 °C, the tensile strength of the investigated alloy rises with the increase in the ε-Al_3Ni phase's content, while the ductility decreases. In their study, the Ni content ranged from 1% to 4%, which was higher than that in our study. This suggests that a higher Ni content (Ni > 1%) can further enhance the alloy's strength but severely compromise its ductility (the elongation dropped to less than 1%). They consider that the ε-Al_3Ni's elastic modulus is significantly higher than that of α-Al. During the alloy deformation process, the ε-Al_3Ni phase will bear more stress until it breaks. Therefore, alloys with a high ε-Al_3Ni phase content will have higher strength. In addition, they also found that the average size of the ε-Al_3Ni phase enlarges with the rise in Ni content, indicating that the brittle Ni-rich phases will further weaken the ductility of the alloy. In a study by Stadler et al. on the effect of Ni addition on the elevated temperature performance of Al-Si alloys, they observed that as the Ni content increases, the alloy's strength enhances [34]. They attribute the strengthening mechanism to the transfer of loads to the harder ε-Al_3Ni phase in the coarse two-phase system structure. Simultaneously, the presence of the ε-Al_3Ni phase contributes to stabilizing the continuity of the eutectic silicon network, thereby enhancing the alloy's overall strength.

If the Ni addition in the alloy is further increased, more Ni-rich phases will form, and the size of these phases will increase. The Ni-rich phase with high temperature stability will further enhance the alloy's elevated temperature strength until it approaches a limit value. And, the strength at room temperature may begin to decline [21]. However, concurrently, the coarse, brittle and hard Ni-rich phases will fracture the alloy matrix and drastically reduce the alloy's plasticity. This phenomenon has been observed in studies on variations in Ni content in A-Si-Mg-Cu alloys [20,33,35]. Insufficient plasticity can affect the forming, processing and reliability of the alloy in service. Therefore, it is generally desirable for alloy materials to possess higher strength while preserving a specific degree of ductility. In this study, a sharp decline in ductility is observed when the Ni content surpasses 0.6%. At the Ni content of 0.6%, the alloy exhibits peak ductility at both room temperature and 250 °C, reaching 2.6% and 4.3%, respectively. At the same time, the alloy demonstrates high strength at both room temperature (391 MPa) and 250 °C (247 MPa), outperforming many heat-resistant alloys within the Al-Si-Cu-Mg system, as illustrated in Table 2. This means that the addition of 0.6Ni to the investigated alloy could attain a favorable combination of ductility and strength.

During the alloy melting and filling process, surface oxide films could get entrained into the interior of the melt as bifilms. These entrainment defects have an adverse impact on the mechanical properties of the alloy [36]. For this study, the alloy melt was refined using high-purity Ar (99.99%) for rotational degassing before pouring, which could reduce the content of oxides [37]. All samples were prepared using exactly the same process. The impact of possible oxidation on each sample should be the same, not a variable, and we conducted repeated experiments to mitigate the impact of random fluctuations. Therefore, it does not affect the final conclusion mentioned above.

Table 2. Room temperature and high temperature strength of Al-Si-Cu system heat-resistant alloy.

Alloy	State	UTS at 25 °C /MPa	UTS at 250 °C /MPa	References
Al-7Si-1Cu-0.5Mg-0.28V-0.18Ti-0.15Zr	T6	311	205	Adapted from Ref. [38]
Al-8Si-2Cu-0.15Zr	T6	435	177	Adapted from Ref. [39]
Al-9Si-1.65Cu-0.45Mg-0.3Mo-0.1Ti	T6	350	87	Adapted from Ref. [40]
Al-11.1Si-3.14Cu-0.9Mg-2.15Ni-0.46Mn-0.19Ti-0.25Ce	T6	280	210	Adapted from Ref. [41]
Al-8.59Si-0.79Cu-0.37Mg-0.12Ti-0.14Zr	T6	374	177	Adapted from Ref. [42]
Al-6.15Si-2.12Cu-0.44Mg-0.72Fe-0.4Zn-0.13Mn-0.05Cr	T6	252	154	Adapted from Ref. [43]
Al-11Si-3Cu-0.2Sm	As cast	-	201.5	Adapted from Ref. [44]
Al-12Si-0.9Cu-0.8Mg-0.5Mn-0.4Fe-0.3Zn-0.2Ti-4Ni	As cast	208	187	Adapted from Ref. [31]
Al-12.8Si-2Cu-1.6Mg	As cast	278.7	199	Adapted from Ref. [45]
Al-12Si-4Cu-1.2Mn	T6	-	191.9	Adapted from Ref. [46]
Al-7Si-1.5Cu-0.4Mg-0.3Mn-0.1RE-0.6Ni	T6	391	247	This work

4. Conclusions

This paper studies the effect of different Ni content on the microstructure and mechanical performance at room temperature and 250 °C of the Al-7Si-1.5Cu-0.4Mg-0.3Mn-0.1RE alloy at low Ni content (<1 wt.% Ni). The primary conclusions can be summarized as follows:

(1) As the Ni content increases, the types of Ni-rich phases undergo some change, and the types of Ni-rich phases are correlated with the Ni/Cu ratio. At low Ni content, the predominant Ni-rich phase is primarily γ-Al_7Cu_4Ni, while at a higher Ni content, δ-Al_3CuNi phases start to appear. In addition, the Ni-rich phases' size also increases with the rise in Ni content.

(2) After T6 treatment, the γ-Al_7Cu_4Ni phase decreases significantly and the ε-Al_3Ni phase increases significantly. Combining the analysis of Ni-rich phase morphology, XRD diffraction results and the distribution pattern of Cu element, it is suggested that the γ-Al_7Cu_4Ni phase undergoes decomposition and a transformation into the ε-Al_3Ni phase during the solution process of the alloy. These ε-Al_3Ni phases are characterized by their small size, typically only a few micrometers, and exhibit a granular or blocky morphology.

(3) Within the investigated range of Ni content, the room temperature mechanical performance of the alloy increases with the rise in Ni content, reaching 405.9 MPa at 0.9% Ni addition, representing a 6.4% improvement compared to the 0% Ni alloy. This enhancement is attributed to the dispersion strengthening effect of the small-sized and well-distributed ε-Al_3Ni phases formed during T6 treatment. The high-temperature strength continues to increase with the Ni content, reaching 261.6 MPa at 0.9% Ni addition, a 16.8% improvement compared to the 0% Ni alloy. The improvement in high-temperature strength is ascribed to the distribution of high-melting-point and stable Ni-rich phases at the grain boundaries, effectively increasing the resistance to dislocation motion at elevated temperatures. At 0.6% Ni content, the alloy achieves a favorable combination of ductility and strength, displaying superior comprehensive mechanical properties compared to many heat-resistant alloys within the Al-Si-Cu-Mg system.

Author Contributions: Conceptualization, S.L.; methodology, S.L. and S.W.; investigation, H.C., J.L. and D.Z.; formal analysis, H.C.; writing—original draft, H.C.; writing—review and editing, S.W., S.L., J.L. and D.Z. All authors have read and agreed to the published version of the manuscript.

Funding: This work was funded by the Project 52205364 and 52175321 supported by the National Natural Science Foundation of China.

Data Availability Statement: The original contributions presented in the study are included in the article/supplementary material, further inquiries can be directed to the corresponding author/s.

Acknowledgments: The authors would also like to express their appreciation to the Analytical and Testing Centre, HUST.

Conflicts of Interest: The authors declare no conflicts of interest.

References

1. Qin, Y.; Yan, Z.; Wu, Q.; Jiang, A.; Li, Y.; Ma, S.; Lü, S.; Li, J. Development of a novel high strength Al-Si-Cu-Ni alloy by combining micro-alloying and squeeze casting. *J. Alloys Compd.* **2023**, *967*. [CrossRef]
2. Zhang, H.; Liu, Y.; Fan, T. Progress and Prospect of Cast Heat-resistant Aluminum Alloy. *Mater. Rev.* **2022**, *36*, 20120048-9.
3. Hernandez-Sandoval, J.; Zedan, Y.; Songmene, V.; Abdelaziz, M.H.; Samuel, F.H.; Garza-Elizondo, G.H. Effect of Minor Addition of Ni and Zr on the High-Temperature Performance of Al-Si-Cu-Mg Cast Alloys. *Int. J. Met.* **2022**, *16*, 1235–1251. [CrossRef]
4. Cho, Y.-H.; Im, Y.-R.; Kwon, S.-W.; Lee, H.-C. The Effect of Alloying Elements on the Microstructure and Mechanical Properties of AI-12Si Cast Alloys. In Proceedings of the Thermec'2003 pt.1, Madrid, Spain, 7–11 July 2003; pp. 339–344.
5. Rohatgi, P.K.; Sharma, R.C.; Prabhakar, K.V. Microstructure and mechanical properties of unidirectionally solidified Al-Si-Ni ternary eutectic. *Met. Trans. A* **1975**, *6*, 569–575. [CrossRef]
6. Moustafa, M.A.; Samuel, F.H.; Doty, H.W. Effect of solution heat treatment and additives on the hardness, tensile properties and fracture behaviour of Al-Si (A413.1) automotive alloys. *J. Mater. Sci.* **2003**, *38*, 4523–4534. [CrossRef]
7. Karamouz, M.; Azarbarmas, M.; Emamy, M. On the conjoint influence of heat treatment and lithium content on microstructure and mechanical properties of A380 aluminum alloy. *J. Mater. Des.* **2014**, *59*, 377–382. [CrossRef]
8. Irizalp, S.G.; Saklakoglu, N.J.E.S.; Technology, A.I.J. Effect of Fe-rich intermetallics on the microstructure and mechanical properties of thixoformed A380 aluminum alloy. *Eng. Sci. Technol. Int. J.* **2014**, *17*, 58–62.
9. Hwang, J.Y.; Banerjee, R.; Doty, H.W. The effect of Mg on the structure and properties of Type 319 aluminum casting alloys. *J. Acta Mater.* **2009**, *57*, 1308–1317. [CrossRef]
10. Li, J.; Pan, Y.; Wu, S.; Chen, L.; Guo, W.; Li, S.; Lü, S. Precipitates strengthening mechanism of a new squeeze-cast Al–Cu–Li–Mn alloy with high strength and ductility. *J. Mater. Res. Technol.* **2023**, *25*, 1334–1343. [CrossRef]
11. Asghar, Z.; Requena, G.; Boiler, E. Three-dimensional rigid multiphase networks providing high-temperature strength to cast AlSi10Cu5Ni1-2 piston alloys. *J. Acta Mater.* **2011**, *59*, 6420–6432. [CrossRef]
12. Asghar, Z.; Requena, G.; Degischer, H.P. Three-dimensional study of Ni aluminides in an AlSi12 alloy by means of light optical and synchrotron microtomography. *J. Acta Mater.* **2009**, *57*, 4125–4132. [CrossRef]
13. Asghar, Z.; Requena, G.; Kubel, F. The role of Ni and Fe aluminides on the elevated temperature strength of an AlSi12 alloy. *J Mater. Sci. Eng. A Struct. Mater. Prop. Misrostruct. Process.* **2010**, *527*, 5691–5698. [CrossRef]
14. Asghar, Z.; Requena, G.; Zahid, G.H. Effect of thermally stable Cu- and Mg-rich aluminides on the high temperature strength of an AlSi12CuMgNi alloy. *J. Mater. Charact.* **2014**, *88*, 80–85. [CrossRef]
15. Li, Y.; Yang, Y.; Wu, Y.; Wang, L.; Liu, X. Quantitative comparison of three Ni-containing phases to the elevated-temperature properties of Al–Si piston alloys. *Mater. Sci. Eng. A* **2010**, *527*, 7132–7137. [CrossRef]
16. Farkoosh, A.R.; Javidani, M.; Hoseini, M.; Larouche, D.; Pekguleryuz, M. Phase formation in as-solidified and heat-treated Al–Si–Cu–Mg–Ni alloys: Thermodynamic assessment and experimental investigation for alloy design. *J. Alloys Compd.* **2013**, *551*, 596–606. [CrossRef]
17. Guo, Y.C.; Gao, X.S.; Xia, F.; Ma, Z.J.; Yang, W.; Yang, Z.; Li, J.P. Phase Transformation of Nickel-Rich Phases in Al-Si Alloy Under Thermal Exposure. *Adv. Eng. Mater.* **2021**, *23*, 2000814. [CrossRef]
18. Liu, Y.Y.; Jia, L.A.; Wang, W.B.; Jin, Z.H.; Zhang, H. Effects of Ni content on microstructure and wear behavior of Al-13Si-3Cu-1Mg-xNi-0.6Fe-0.6Mn alloys. *Wear* **2022**, *500*, 204365. [CrossRef]
19. Suwanpreecha, C.; Pandee, P.; Patakham, U.; Limmaneevichitr, C. New generation of eutectic Al-Ni casting alloys for elevated temperature services. *J Mater. Sci. Eng. A Struct. Mater. Prop. Misrostruct. Process.* **2018**, *709*, 46–54. [CrossRef]
20. Feng, J.; Ye, B.; Zuo, L.; Qi, R.; Wang, Q.; Jiang, H.; Huang, R.; Ding, W. Effects of Ni content on low cycle fatigue and mechanical properties of Al-12Si-0.9Cu-0.8Mg-xNi at 350 °C. *Mater. Sci. Eng. A* **2017**, *706*, 27–37. [CrossRef]
21. Zhang, S.N.; Pan, L.W.; Huang, D.L.; Dong, Q.; Hu, Z.L. Effect of Nickel Alloying and Mechanical Stirring on the Microstructure and Mechanical Properties of Al-10% Si-5% Cu Alloy. *Met. Sci. Heat Treat.* **2020**, *61*, 769–776. [CrossRef]
22. Zhong, G.; Wu, S.; Jiang, H.; Wan, L. Microstructure feature of high silicon content aluminum alloys with RE. *Huazhong Keji Daxue Xuebao (Ziran Kexue Ban)/J. Huazhong Univ. Sci. Technol. (Nat. Sci. Ed.)* **2010**, *38*, 29–32.
23. Biswas, P.; Patra, S.; Roy, H.; Tiwary, C.S.; Paliwal, M.; Mondal, M.K. Effect of Mn Addition on the Mechanical Properties of Al–12.6Si Alloy: Role of $Al_{15}(MnFe)_3Si_2$ Intermetallic and Microstructure Modification. *Met. Mater. Int.* **2021**, *27*, 1713–1727. [CrossRef]
24. Kishor, M.; Chopra, K.; Ayyagari, K.P.R. Tackling Fe-rich Intermetallics in Al-Si Alloy: A Critical Review. *Trans. Indian Inst. Met.* **2023**. [CrossRef]
25. Qian, D.L.; Lan, K.; Yang, Y.T. The Effect of Solution Temperature on Microstructure Evolution and Mechanical Properties of a Low-Silicon Cast Aluminum Alloy Containing Mn. *Int. J. Met.* **2023**. [CrossRef]
26. Zheng, J.L.; Pang, Y.F.; Shi, H.J.; Hu, W.R.; Liu, H.; Du, X.D. Effect of Mn and B Addition on the Microstructure and Properties of Al-Si-Cu-Mg Cast Alloy. *Int. J. Met.* **2023**. [CrossRef]

27. *GB/T 228.1-2021*; Metallic materials - Tensile testing - Part 1: Room temperature test methods. State Administration for Market Regulation: Beijing, China, 2021.
28. *GB/T 228.2-2015*; Metallic materials - Tensile testing - Part 2: High temperature test methods. General Administration of Quality Supervision, Inspection and Quarantine of the People's Republic of China: Beijing, China, 2015.
29. Liao, H.; Liu, Q.; Li, G.; Dixit, U.S. Effect of Ni Addition on the Solidification Process and Microstructure of Al-12% Si-4% Cu-1.2% Mn-x% Ni Heat-Resistant Alloys. In *Proceedings of the Light Metals*; Springer: Berlin/Heidelberg, Germany, 2018; pp. 267–278.
30. Yang, Y.; Li, Y.-G.; Liu, X.-F. Evolution of the rich-nickel intermetallics of high-iron Al-Si piston alloy. *Cailiao Rechuli Xuebao/Trans. Mater. Heat Treat.* **2011**, *32*, 86–89.
31. Yang, Y.; Yu, K.; Li, Y.; Zhao, D.; Liu, X. Evolution of nickel-rich phases in Al–Si–Cu–Ni–Mg piston alloys with different Cu additions. *Mater. Des.* **2012**, *33*, 220–225. [CrossRef]
32. Zuo, L.; Ye, B.; Feng, J.; Xu, X.; Kong, X.; Jiang, H. Effect of delta-Al_3CuNi phase and thermal exposure on microstructure and mechanical properties of Al-Si-Cu-Ni alloys. *J. Alloys Compd. Interdiscip. J. Mater. Sci. Solid-State Chem. Phys.* **2019**, *791*, 1015–1024. [CrossRef]
33. Zuo, L.; Ye, B.; Feng, J.; Zhang, H.; Kong, X.; Jiang, H. Effect of ε-Al_3Ni phase on mechanical properties of Al–Si–Cu–Mg–Ni alloys at elevated temperature. *Mater. Sci. Eng. A* **2020**, *772*, 138794. [CrossRef]
34. Stadler, F.; Antrekowitsch, H.; Fragner, W.; Kaufmann, H.; Uggowitzer, P.J. The effect of Ni on the high-temperature strength of Al-Si cast alloys. In *Materials Science Forum*; Trans Tech Publications Ltd.: Bäch, Switzerland, 2011; pp. 274–277.
35. Liao, H.; Li, G.; Liu, Q. Ni-Rich Phases in Al-12%Si-4%Cu-1.2%Mn-x%Ni Heat-Resistant Alloys and Effect of Ni-Alloying on Tensile Mechanical Properties. *J. Mater. Eng. Perform.* **2019**, *28*, 5398–5408. [CrossRef]
36. Olofsson, J.; Bogdanoff, T.; Tiryakioğlu, M. On revealing hidden entrainment damage during in situ tensile testing of cast aluminum alloy components. *Mater. Charact.* **2024**, *208*, 113647. [CrossRef]
37. Huang, Y.; Gao, X.; Liu, Y.; Sheng, Z.; Fan, X. A qualitative and quantitative investigation of nonmetallic inclusions in molten Al–Mg, Al–Cu, and Al–Zn–Mg–Cu alloys. *J. Mater. Res. Technol.* **2024**, *28*, 87–96. [CrossRef]
38. Kasprzak, W.; Amirkhiz, B.S.; Niewczas, M. Structure and properties of cast Al–Si based alloy with Zr–V–Ti additions and its evaluation of high temperature performance. *J. Alloys Compd.* **2014**, *595*, 67–79. [CrossRef]
39. Mondol, S.; Bansal, U.; Singh, M.P.; Dixit, S.; Mandal, A.; Paul, A.; Chattopadhyay, K.J.M. Microstructure-strength correlations in Al-Si-Cu alloys micro-alloyed with Zr. *Materialia* **2022**, *23*, 101449. [CrossRef]
40. Morri, A.; Ceschini, L.; Messieri, S.; Cerri, E.; Toschi, S.J.M. Mo Addition to the A354 (Al–Si–Cu–Mg) casting alloy: Effects on microstructure and mechanical properties at room and high temperature. *Metals* **2018**, *8*, 393. [CrossRef]
41. Liu, H.Q.; Pang, J.C.; Wang, M.; Li, S.X.; Zhang, Z.F. Effect of temperature on the mechanical properties of Al–Si–Cu–Mg–Ni–Ce alloy. *Mater. Sci. Eng. A* **2021**, *824*, 141762. [CrossRef]
42. Liu, G.; Blake, P.; Ji, S. Effect of Zr on the high cycle fatigue and mechanical properties of Al-Si-Cu-Mg alloys at elevated temperatures. *J. Alloys Compd. Interdiscip. J. Mater. Sci. Solid-State Chem. Phys.* **2019**, *809*, 151795. [CrossRef]
43. Aziz, A.M.; Omar, M.Z.; Samat, S.; Mohamed, I.F.; Sajuri, Z.; Baghdadi, A.H. Microstructural and Tensile Behavior of a Thixoformed Al–Si–Cu–Mg Given T5 and T6 Heat Treatments Tested at Room and Elevated Temperatures. *Int. J. Met.* **2023**, 1–14. [CrossRef]
44. Shuai-bo, Z.; Yong, S.; Wen-gang, G. Effects of rare earth elements on microstructure and tensile properties of Al-Si-Cu alloy at 250 °C. *J. China Foundry* **2021**, *18*, 474–480. [CrossRef]
45. Zuo, L.; Ye, B.; Feng, J.; Kong, X.; Jiang, H.; Ding, W. Effect of Q-$Al_5Cu_2Mg_8Si_6$ phase on mechanical properties of Al-Si-Cu-Mg alloy at elevated temperature. *J. Mater. Sci. Eng. A Struct. Mater. Prop. Misrostruct. Process.* **2017**, *693*, 26–32. [CrossRef]
46. Liao, H.; Tang, Y.; Suo, X.; Li, G.; Hu, Y.; Dixit, U.S.; Petrov, P. Dispersoid particles precipitated during the solutionizing course of Al-12 wt %Si-4 wt%Cu-1.2 wt%Mn alloy and their influence on high temperature strength. *J. Mater. Sci. Eng. A Struct. Mater. Prop. Misrostruct. Process.* **2017**, *699*, 201–209. [CrossRef]

Disclaimer/Publisher's Note: The statements, opinions and data contained in all publications are solely those of the individual author(s) and contributor(s) and not of MDPI and/or the editor(s). MDPI and/or the editor(s) disclaim responsibility for any injury to people or property resulting from any ideas, methods, instructions or products referred to in the content.